The impact of tropical cyclones on potential offshore wind farms

The impact of tropical cyclones on potential offshore wind farms

Kanzis L. Mattu[1], Hannah Bloomfield[2], Simon Richard Thomas[3], Oscar Martínez-Alvarado[1] and Osvaldo Rodríguez-Hernández[4],

March 11, 2022

[1] National Centre for Atmospheric Science, University of Reading, Department of Meteorology, Harry Pitt Building, Whiteknights Road, Earley Gate, Reading, RG6 6ES, United Kingdom.

[2] Department of Meteorology, University of Reading, Meteorology Building, Whiteknights Road, Earley Gate, RG6 6ET, United Kingdom. Now at: School of Geographical Sciences, University of Bristol, United Kingdom.

[3] L'Institut de Recherche en Astrophysique et Planétologie, 9 Avenue du Colonel Roche, 31400 Toulouse, France.

[4] Instituto de Energías Renovables, Universidad Nacional Autónoma de México, Priv. Xochicalco s/n, Col. Centro, CP 62580, Temixco, Morelos, Mexico.

Abstract

The climate crisis has led to an increased interest in renewable energy, and in wind energy in particular. Wind farms with the largest generating potential are generally located offshore. In this study we consider the case of Mexico, a sub-tropical country in North-America. Due to Mexico's location, offshore wind farms (OWF) would be at risk of damage from strong winds associated with tropical cyclones (TCs) in both the Pacific and the Gulf of Mexico basins. Thus, here we ask whether there are any regions in Mexico combining a high generating potential and a low risk from tropical cyclones. To answer this question, the ERA5 reanalysis has been used to identify two sites on the Pacific coast and two sites in the Gulf of Mexico with high wind power potential. Then, using the ERA5 reanalysis and TC best-track observational data, the potential effects of four major hurricanes and the climatological hazard posed by TC-related damaging winds on OWFs at those sites have been investigated. The return period for TCs with near-surface winds exceeding 50 m s^{-1}, a threshold associated with increased structural damage likelihood, has been estimated at as low as 8 years for the Gulf of Mexico and above 64 years for Pacific coast. Therefore, in terms of the magnitude of the TC-related hazard, the Pacific coast sites are found to be preferred as locations for the development of OWFs. These results are relevant for any planning of offshore wind energy in Mexico, and the methodology applicable to any other sub-tropical region in which the risk of tropical cyclones is present.

Keywords

Extreme wind conditions; Wind power; Mexico; Climate risk; Offshore wind; Natural Hazards

1 Introduction

Global population growth, coupled with industrial expansion has increased the large-scale demand for energy. At present, the most technologically developed and cost-effective route to transform the energy sector in response to the climate crisis is through installing renewable energy generation Quaschning (2019). The tropics are a favourable region for wind energy production as they are characterised by relatively consistent annual mean near-surface wind speeds, hence making them a suitable location for harnessing wind energy Clausen et al. (2007). One sub-tropical country which shows excellent potential for wind energy generation is Mexico (Martínez Narro et al., 2014; Cancino-Solórzano et al., 2011). Mexico's geography is associated with great potential for the production of renewable energy such as solar and wind, the latter particularly in many coastal regions (Martínez Narro et al., 2014). In 2020, 27% of Mexico's electricity was produced from clean energy sources, with 8.8% of that from hydro, 1.5% from geothermal, 5.9% from wind and 4.2% from solar PV de México Secretaría de Energía (2020). Previous studies have shown that the country's wind power potential is predominantly located in offshore coastal regions (Cancino-Solórzano et al., 2011). From January to April the greatest wind energy potential is located in the southeast of Mexico with values greater than 800 W/m^2

Gallardo et al. (2020). This region is considered one of the best regions globally to exploit wind energy due to the strong and persistent Tehaunos winds channeling through the gap in the mountains Jaramillo et al. (2004). Baja California (BC) and the northeastern coast of Mexico have also been identified as areas of high wind energy potential Gallardo et al. (2020). As a whole, the country has the potential to install 40 GW of wind power generation Cancino-Solórzano et al. (2011). Baja California Sur was found to be a suitable location to exploit wind energy as the unique geography between the Pacific ocean and Gulf of California provides viable wind speeds throughout the year Jaramillo et al. (2004). There is a seasonal variation in the wind potential across Mexico, with a decrease in the southeast and an increase in the northeast region in the summer Gallardo et al. (2020). Whilst the southeast may produce the highest wind energy potential (predominantly in the winter), there are other regions of Mexico that are viable for harnessing wind energy such as the Baja California peninsula, Tamaulipas and the Yucatan peninsula, which is why this study has chosen to analyse the aforementioned regions shown in Fig. 1. Furthermore, due to the seasonality present within the wind climatology, these other regions of Mexico would be of increased importance for wind energy production when there is not sufficient wind present in the southeast Thomas et al. (2020).

Although an offshore wind farm (OWF) in the region is also exposed to other geophysical and meteorological hazards, such as extreme wave heights Gkoumas (2010); Malhotra (2007), one of the main meteorological concerns with constructing OWFs throughout the tropics is the destructive force of tropical cyclones (TCs) on the offshore wind turbines (OWTs) and the OWF infrastructure Worsnop et al. (2017). Tropical cyclones (TCs) are intense, warm-cored cyclonic vortices that develop over the warm tropical oceans. (i.e. 23° N to 23°S) Chan and Kepert (2010). TCs occur globally within seven basins, two of which are relevant for the area of study, namely the Eastern North Pacific and the North Atlantic. In these basins, tropical cyclones are classified based on 1-minute average 10-m winds into three categories: (a) Tropical depression, with maximum wind speed less than 17.5 m s^{-1}; (b) tropical storms, with maximum wind speed between 17.5 m s^{-1} and 33 m s^{-1}, and (c) hurricanes, with maximum wind speed in excess of 33 m s^{-1}. and have associated wind speeds which can surpass 70 m s^{-1} Neumann (2017). The strongest winds and torrential rains in a TC occur mainly in the TC eye wall. This is the region of rapidly rotating surface winds that surround the relatively calm *eye*, located in the centre of the TC;Wang and Wu (2004)). Mexico is vulnerable to landfalling TCs on both its Pacific and Atlantic coasts, with over 70% occurring between August and October, peaking in September Breña-Naranjo et al. (2015). Research on hurricane climatology has shown that 9% of all hurricane activity on the Atlantic coast and 18% on the Pacific coast around Mexico between 1951 and 2000 made landfall Jáuregui (2003). Furthermore, while there were more Category 5 hurricanes on the Atlantic than the Pacific coast, both coasts were affected by the same number of major hurricanes (Category 3-5) Jáuregui (2003). Thus, to successfully make progress on the use of wind energy in Mexico, it is necessary to consider and understand the risks that meteorological phenomena such TCs may have on OWFs.

For a TC to be classified as a hurricane the sustained 10-m winds must be greater than

33 m s^{-1} Taylor et al. (2010). This poses a challenge to OWFs as the typical cut-out speed for a wind turbine is 25 m s^{-1}. Furthermore, the potential for damage in OWF increases exponentially with increasing wind speed. Therefore strong wind-gusts could cause substantial problems Worsnop et al. (2017). If the cut-out speed of a wind turbine is exceeded the mechanical break will engage to attempt to stop the turbine from rotating. If the turbine continues to rotate, then two subsequent implications could occur. A fire could start within the rotor due to mechanical break being engaged while the turbine is rotating past the cut-out speed, and/or the blades will spin too fast causing an extreme load on the blades, leading to eventual breakage and possible collapse of the structure Hong and Möller (2012). The supplementary consequences of the possible damage include costly repairs to the OWT. Due to their location, OWFs are more difficult to access than onshore wind farms, and so would require specialised ships and cranes to perform repairs Hallowell et al. (2018). Depending on the widespread damage to the OWF there is also the risk of decreased energy production Zhang et al. (2018).

Previous studies have investigated the impact of tropical cyclone damage on onshore wind turbines from an engineering perspective. Martín del Campo et al. Martín del Campo et al. (2021) found that modifying the structure of onshore turbines by adding passive damping systems would reduce turbine fragility by 80%. Jaimes et al. Jaimes et al. (2020) employ a probabilistic risk assessment to explore the economic impact of tropical cyclones on onshore wind farms in Mexico. A key limitation of these studies is the limited amount of meteorological data that is available for the assessment. To further add to the findings of these studies, this paper presents a method to use high resolution meteorological data to investigate the impact of tropical cyclones on offshore wind farms across a multi-decadal period.

The aim of the paper is to quantify the potential hazard posed by high wind speeds associated with tropical cyclones affecting those regions in Mexico which are favourable for offshore wind energy production. This is executed through identifying regions of Mexico which present a viable capacity factor (CF), subsequent analysis of four major hurricanes which have affected each selected site and, finally, a return period analysis of historical TCs in Mexico. The rest of the paper is structured as follows: Section 2 describes the data and methodology used. In Section 3 the results of the wind power climatology and the selection of OWF sites are discussed. The four case studies are discussed in Section 4. The long term assessment of TC return periods is presented in Section 5. Finally, Section 6 draws conclusions of the work.

2 Data and Methodology

2.1 TC Best-Track observations

The International Best Track Archive for Climate Stewardship (IBTrACS) dataset Knapp et al. (2010) was used to compute TC return periods and to perform bias correction on ERA5-derived wind speeds (see Section 2.2). IBTrACS is a standardised set of observations of Best-Track data from several international meteorological agencies Knapp et al. (2010). IBTrACS contains multiple parameters including TC centre location, maximum sustained wind speed

and minimum mean sea-level pressure Kruk et al. (2010).

In this study we use TC location and the maximum sustained 10-m wind speed associated with each TC time step for hurricane seasons within the period between 1979 and 2019, inclusive. The original IBTrACS data has been processed in the same way as in Hodges et al. (2017), i.e., wind speeds recorded in knots have been converted to metres per second. While post-processing during the original IBTrACS compilation is used to minimise differences in wind-averaging periods used by different agencies, inconsistencies arising from the conversion might remain. However, for the computation of return periods in this work only data for the eastern Pacific and the North Atlantic are used, which minimises these inconsistencies as these data are all recorded by the Regional Specialized Meteorological Center in Miami using a 1-min averaging period.

2.2 ERA5 reanalysis data

The European Centre for Medium-Range Weather Forecasts (ECMWF) fifth generation ReAnalysis (ERA5) Hersbach et al. (2020) has been used to provide an estimation of the mean wind resource during hurricane season and to analyse the statistics of near-surface wind speeds in the vicinity of a TC. ERA5 is the latest atmospheric reanalysis produced by ECMWF, available through the Copernicus Climate Change Service. ERA5 has a horizontal resolution equivalent to 31 km grid spacing and 137 vertical levels up to 0.01 hPa (80 km). The ERA5 fields are stored at an hourly temporal resolution. In this study the ERA5 100-m hourly horizontal wind components were used to compute 100-m horizontal wind speed as an estimate of wind speed at hub height, typically in the range between 70 m to 120 m Clausen et al. (2007); Olauson (2018). To provide an estimation of the mean wind resource during hurricane season, the hourly ERA5-derived 100-m wind speed was converted into CF using the power curve of a Class I Enercon E70 2.3MW wind turbine (following Bloomfield et al. Bloomfield et al. (2020) who demonstrated this turbine to be an appropriate choice for offshore wind farm locations across Europe). 100-m wind speeds are chosen for the analysis as they are the closest outputs available to a modern offshore hub-height, which can be up to 200-m. The analysis with 100-m wind speeds therefore presents a lower bound on potential damage. To analyse the statistics of near-surface wind speed in the vicinity of a TC, a footprint approach has been taken following Roberts et al. Roberts et al. (2014) (see Section 2.4).

A potential caveat in the use of reanalysis data for wind energy studies is that near-surface wind fields are known to be underestimated by ERA5, e.g., over Mexico Thomas et al. (2020) and Europe Bloomfield et al. (2020). The effect of reanalyses biases has been found to be generally less important as the averaging time period increases (e.g., Cannon et al., 2015b; Morales-Ruvalcaba et al., 2020). Therefore, bias correction was not performed for the estimation of the mean wind resource during hurricane season. However, Hodges et al. Hodges et al. (2017) showed that near-surface wind speed during the occurrence of TCs is severely underestimated by reanalyses, a result that can be extended to ERA5 as well (not shown). Therefore, bias correction is important for the analysis of wind speed statistics during the occurrence of TCs.

In this work quantile mapping (e.g., Cannon et al., 2015a) was used as a bias correction method. Maximum 10-m wind speeds associated with all northern hemisphere TCs during the period between 1979 and 2019 as recorded by IBTrACS were used to construct a target cumulative distribution function (CDF). The corresponding ERA5-derived maximum 10-m wind speeds were used to construct the CDF to train the bias correction method. Bias correction was then applied to ERA5 100-m wind speed during the life cycles of the four case studies to produce a better estimate of hub-height wind speed values around cyclones' centres. While the bias correction method was trained on 10-m wind speed and applied to 100-m wind speed, the error arising from this procedure is deemed to be small in comparison with the error that would arise from not using bias correction at all. We note that even with the bias correction, the resulting wind speeds are still sometimes lower than those reported by IBTRACS. These results therefore present a lower-bound on potential wind speed damage to OWTs during TCs.

2.3 Cyclone tracking

ERA5 TC tracks have been used to construct the CDF to train the bias correction method (see Section 2.2) and to construct the wind speed footprints in the case-study TCs. An objective feature-tracking algorithm Hodges et al. (2017); Hodges (1994, 1995, 1999) has been used to identify TCs within the ERA5 data and to track the path of the cyclones' centres. The cyclone tracking is based on the search for local maxima in the vertically averaged 850–600-hPa relative vorticity filtered to retain total wavenumbers between 6 and 63 at 6-hourly time steps. We acknowledge that despite filters being applied we are including tropical disturbances through to hurricanes. Only tracks lasting more than two days are retained for further analysis. The full description of this method can be found in Hodges et al. Hodges et al. (2017). As part of the algorithm the maximum 10-m wind speed in a 1000-km radius from the cyclone's centre is attached to the TC track at each 6-hourly time step. These maximum wind speed values constitute the underlying data to construct the quantile mapping training CDF used for bias correction.

2.4 Wind speed footprints

To investigate the maximum near-surface wind speeds associated with TCs the wind-storm footprint method devised by Roberts et al. Roberts et al. (2014) for the case of extratropical cyclones has been employed with slight modifications. In this work, the TC wind speed footprint is given by the maximum hourly 100-m wind speed at each grid point within a circular area of influence around the TC centre over the entire TC life-cycle. The area of influence in studies of precipitation associated with TCs has been defined as a 5 geodesic degree area around the cyclone centre Franco-Díaz et al. (2019). However, in this work a 7.5 geodesic degree radius has been used, as preliminary analysis has shown this to be more suitable for the 100-m wind field. The hourly temporal resolution was used when creating the footprints to capture the highest-frequency variability available from the reanalysis dataset. Moreover, using hourly data is also

important considering that TCs can undergo rapid intensification, advancing from a tropical storm to a major hurricane over a timescale of a few hours.

2.5 Tropical cyclone return periods

Return periods have been estimated as the inverse of the probability of the next occurrence of a given event Wilks (2011). Two types of events have been considered: (i) TCs making landfall in Mexico, and (ii) TCs with 10-m wind maxima above a given threshold occurring in the vicinity of a potential OWF site. The probability of the next occurrence of a TC has been modelled using the Poisson distribution, which has been used for this purpose in previous studies (e.g., Georgiou et al., 1983; Katz, 2002; Parisi and Lund, 2008). The Poisson distribution depends on a single parameter, which can be interpreted physically as the average occurrence rate Wilks (2011). Here, the average occurrence rate at a given location is estimated by the TC track density at that location, i.e. the number of TC tracks passing through a 2 geodesic degree spherical cap centred on the location of interest. The Poisson distribution is used to compute the probability of at least one TC occurring in a given year.

The return period for the first event type can be determined by computing the track density considering only TCs that made landfall in Mexico during the 41-year period included in this work. On the other hand, computing the return period of TCs with 10-m wind maxima above a given high wind speed threshold is less straightforward as the sample size for such extreme events becomes very small. Therefore, to estimate the desired probability, the probability derived from the track density was weighted by the probability of a cyclone bearing winds above the specified threshold. Thus, the desired probability is firstly estimated by

$$P(\text{TC and } u > u_{\text{thresh}}) = P(u > u_{\text{thresh}}|TC) \cdot P(\text{TC}), \tag{1}$$

where $P(\text{TC})$ is the track-density-derived probability and $P(u > u_{\text{thresh}}|TC)$ is the probability of the wind speed threshold being surpassed given that a TC is occurring. This probability can be estimated through simulated wind fields for a given site Jaimes et al. (2020); Jaimes and Niño (2018). This approach is most effective when the location of the assets is known such as for the case of households Jaimes and Niño (2018) or onshore wind farms Jaimes et al. (2020). However, while in this work we consider potential sites for the installation of OWFs, these sites are only hypothetical as no OWFs are currently in operation in Mexico. Thus, in this work this probability was estimated empirically using the 10-m wind maximum values for all cyclones passing within a 3.75 geodesic degree spherical cap centred around the locations of the potential OWF sites. The size of the spherical cap was chosen to be consistent with the findings regarding the wind speed footprints (see Section 2.4). The wind maximum values were obtained from the IBTrACS dataset.

To ensure that the probability estimated by Eq. (1) was consistent with observations, it was tested using a two-tailed test based on the binomial distribution for the probability of either having or not having TC-related wind speeds surpassing the threshold in each of the four

regions. The observations used were the tracks actually satisfying these conditions. If the null hypothesis, i.e. that the probability given by Eq. (1) is consistent with the observed number of cyclones surpassing a given threshold, was rejected at a 10% level a correction was applied. In general, when the null hypothesis was rejected, it was because the estimated probability was not sufficiently high. Therefore, the estimated probability was corrected upwards by increasing it by a tenth of the original estimated probability in a maximum of ten steps (i.e. the final probability could only be double the original).

3 Potential offshore wind farm sites

This study focuses on the following four offshore sites in Mexico, which have been identified as having high wind resource potential Canul-Reyes (2020); Hernández-Escobedo et al. (2010): the Yucatan peninsula (YUC), Tamaulipas (TMPS), the Isthmus of Tehuantepec (IOT) and the Baja California peninsula (BC). The first two sites, in the Gulf of Mexico, were identified by Canul-Reyes Canul-Reyes (2020), who in addition to wind energy production potential included factors such as the distance to the coast, sea floor depth and the location of biodiversity protection areas, to the determine the feasibility of a given site. The other two sites, on the Mexican Pacific coast, have been chosen based on previous wind resource assessment work Hernández-Escobedo et al. (2010).

The mean CF during hurricane season (1 June–30 November) derived from ERA5 reanalysis data between 1980 and 2017 and the locations of the chosen OWF sites are shown in Fig. 2. The CF values show that the potential OWF sites in BC, TMPS, IOT and YUC are all sites which have mean CF greater than 20% within their neighbourhoods. IOT has the highest mean CF during hurricane season of over 40%, and Baja California and Tamaulipas have some areas of 25–30% and the north-west of the Yucatan peninsula has a CF of 20–25%. Figure 2 gives an overview of the CF in Mexico but to understand the CF evolution throughout the year at a particular site of interest the minimum, median and maximum values of the monthly mean CF are displayed in Fig. 3. Analysis of the monthly evolution of CF gives a further insight into previous studies, which have only assessed the mean annual wind speed and have based the wind energy potential on that value. For example, Hernández-Escobedo et al. Hernández-Escobedo et al. (2010) concluded that that the majority of Mexico had an annual mean CF of 19% allegedly making most regions viable for wind energy production. However, the data presented in Fig. 3 shows that there is a strong seasonal cycle in the wind climatology with a maximum in winter and a minimum in summer, explaining why initially it may appear that all regions are viable locations for wind energy production. However, the CF ideally must be greater than 19% throughout the year to be worthwhile financially and to consistently produce energy Blanco (2009).

The seasonal cycle is most prominent in IOT due to the funnelling effect of air from cold surges moving south from the US during winter and being accelerated through the gap in the topography i.e. between the Sierra Madre de Oaxaca to the west and the Sierra Madre

de Chiapas to the east Maldonado et al. (2018), in a phenomenon known as the Tehuanos winds Hurd (1929); Steenburgh et al. (1998); Prósper et al. (2019). From the data presented, Tamaulipas has the most viable CF throughout the year, in agreement with the findings of Carrasco et al. Carrasco-Díaz et al. (2015), who investigated the development of onshore wind farms around the State of Tamaulipas and estimated that the CF in the northern sector of the State was 30%. The minimum, median and maximum values for this site all follow a similar evolution with a maximum in April and a minimum in September with the minimum falling to around 10%. Although IOT presents the highest CF this is highly variable throughout the year Barton et al. (2009); Díaz Méndez et al. (2010) and therefore not as desirable when considering stable energy production. During the months of the hurricane season CFs are generally low. This could be due to high wind speed cut-out associated with the passing TCs, or due to the generally low wind conditions at times when TCs are not present.

4 Case studies

TCs which surpass the wind speed of a Category 2 hurricane on the Saffir-Simpson wind scale Simpson and Riehl (1981) exceed the design limit of turbine standards, as outlined by the International Electrotechnical Commission (Worsnop et al., 2017). An OWT would be likely to collapse if exposed to a Category 5 hurricane Worsnop et al. (2017); Han et al. (2014). TC associated gusts in excess of 70 m s^{-1} have been found to cause structural damage to OWTs e.g. severe aerodynamic loading, ultimately causing turbine components to fail Worsnop et al. (2017). We note this is a general threshold rather than being specific to the ENERCON E70 2.3MW used in this study. In reality the chosen thresholds would be very turbine specific and depend on a number of factors However, unpacking this is beyond the scope of this initial study. In this section a case study analysis of four major hurricanes (two in the Atlantic and two in the Pacific) was completed to investigate the impact of the selected extreme TCs on potential offshore wind farm locations. Hurricanes were chosen based on the premise that each would have impacted at least one of the proposed offshore wind farm sites (see Fig. 2). Using these conditions, the following hurricanes were chosen for analysis: Hurricane Gilbert (1988), Hurricane Wilma (2005), Hurricane Odile (2014) and Hurricane Patricia (2015). The hurricane tracks, the associated 100-m wind speed footprint and areas in which cut-out would have been experienced are shown in Fig. 4. Further details on these hurricanes and the effect of bias correction (described in section 2.2) is illustrated in Table 1, which shows the ERA5-derived maximum 100-m wind speed before and after bias correction and the corresponding 10-m wind speed value reported by NOAA for each case study. The distribution of associated 100-m wind speeds within a 7.5 geodesic degree radius of the track is shown in Figure 5 with selected probabilities displayed in Table 2. The thresholds have been chosen as they represent typical turbine cut-out (25 m s^{-1}), potential structural damage (50 m s^{-1}), and a high possibility of structural damage (70 m s^{-1}). The structural damage thresholds have been chosen based on empirical data on tropical cyclone damage on wind turbines as presented by Hong and Möller

Hong and Möller (2012). Further details on each case are given in Sections 4.1–4.4, followed by a case-study summary in Section 4.5.

4.1 Hurricane Patricia

Hurricane Patricia was a Category 5 hurricane which occurred on 20–24 October 2015 in the Pacific basin. Patricia broke records in the western hemisphere for both minimum central pressure (872 hPa) and maximum sustained surface winds (95 m s^{-1}) (Rogers et al., 2017). The estimated damage inflicted by Patricia was approximately 325 million US dollars. Patricia originated in the Gulf of Tehuantepec close to the proposed IOT site Kimberlain et al. (2016). Patricia intensified to a major hurricane on 22 October 2015, becoming a Category 5 hurricane within a day. Patricia maintained its intensity when taking a turn north-north-eastward and accelerated towards central Mexico. This change of track propagation occurred due to the presence of a trough moving across the Baja California peninsula Kimberlain et al. (2016). Patricia made landfall in central Mexico on 23 October 2015 as a Category 4 hurricane and then quickly began to lose intensity as it travelled inland over the Sierra Madre mountain range. Patricia's path also crossed the proposed TMPS site. The system then dissipated the following day Kimberlain et al. (2016).

Figure 4a shows that there was the potential for high wind speeds in the genesis region of Patricia at the IOT site, with up to 24 hours of cut-out. However, these high wind speeds did not exceed the threshold for potential structural damage. Hurricane Patricia is dissipating as it passes over the TMPS site, and there is only a small region of wind speeds greater than the cutout threshold seen inland of the site.

IBTrACS data show this hurricane had the highest 10-m wind speeds of all chosen case studies (Table 1). However, bias correction only translates the ERA5-derived maximum wind speed in Patricia from 36 m s^{-1} to 63 m s^{-1}, while the corresponding IBTrACS value is 95 m s^{-1} (Table 1). This suggests that even after bias correction (see section 2.2 for details) the 100-m wind speeds associated with hurricane Patricia have been poorly captured by ERA5. This under-representation of extreme near-surface wind speeds has been previously documented by Hodges et al. Hodges et al. (2017). The results from this subsection should therefore be thought of as a lower-bound for the potential damage that a hurricane such as Patricia could cause to the IOT and TMPS sites.

4.2 Hurricane Wilma

Hurricane Wilma was a record-breaking TC which occurred between 16–27 October 2005, passing through the YUC region. Wilma devastated the northeast Yucatan peninsula and was directly responsible for four deaths Pasch et al. (2006). Wilma's minimum central pressure of 882 hPa is the lowest ever recorded in the Atlantic basin, with Hurricane Gilbert (see Section 4.4) in 1988 previously holding the record at 888 hPa Meyer-Arendt (1991). Wilma began as an area of low pressure southwest of Jamaica, which intensified and travelled northwest

Hurricane (Category)	Date	Site Affected	10-m IBTrACS (m s^{-1})	100-m ERA5 (m s^{-1})	100-m BC ERA5 (m s^{-1})
Gilbert (5)	8–19/09/88	YUC TMPS	82	50	95
Wilma (5)	15–25/10/05	YUC	82	51	95
Odile (4)	10–18/09/14	BC	61	34	67
Patricia (5)	20–24/10/15	IOT TMPS	95	36	63

Table 1: For each of the case study hurricanes the following information is provided: the maximum hurricane category reached, the date when the hurricane occurred, the potential offshore wind farm site that would have been affected, the maximum 10-m wind speed as recorded by IBTrACS, the maximum 100-m wind speed estimated by ERA5 with and without bias correction.

across the Yucatan peninsula as a Category 4 hurricane. Figure 4b shows 24–48 hours of potential cut-out would have been experienced at the YUC site associated with Hurricane Wilma. However, as the wind speeds did not exceed 50 m s^{-1} it would be unlikely that there would have been any structural damage. After making landfall Wilma dropped to a Category 2 hurricane and veered northeast towards Florida whilst regaining intensity over the Gulf of Mexico. Wilma made landfall on the west coast of Florida on 24 October Pasch et al. (2006). The gain in intensity resulted in structurally damaging winds (exceeding 70 m s^{-1}) over Florida.

4.3 Hurricane Odile

Hurricane Odile (10–18 September 2014) was the first major hurricane to make landfall in Baja California in 25 years and is tied as the strongest landfalling hurricane to ever affect this region, with estimated insured losses of around 1 billion US dollars Cangialosi and Kimberlain (2015); Murià-Vila et al. (2018). A surface low pressure area formed on 9 September 2014 and became better organised the following day resulting on the formation of a tropical depression, approximately 200 miles southeast of Acapulco, Mexico. Odile reached hurricane status on 13 September 2014 and followed a northwestward path. Odile made landfall in Baja California on 15 September 2014 as a Category 3 hurricane and would have affected the potential BC OWF site. Maximum wind speeds from 25 to 50 m s^{-1} are experienced at the site, with small amounts of cut-out being possible (Fig. 4c). There is only a 0.25% chance of potentially damaging winds happening associated with Hurricane Odile in any region along the track (Table 2), so this is very unlikely to have happened at the BC site. Passage over the rugged terrain of Baja California weakened Odile and the hurricane continued to lose intensity as it travelled further inland before dissipating on 18 September 2014 Cangialosi and Kimberlain (2015).

4.4 Hurricane Gilbert

Hurricane Gilbert was the strongest recorded TC to make landfall in Mexico, causing an estimated 1–2 billion US dollars in damage (in Mexico) Clark (1988) breaking a number of

Hurricane	> 25 ms^{-1}	> 50 ms^{-1}	> 70 ms^{-1}
Gilbert	18.64%	2.39%	0.23%
Wilma	21.3%	3.31%	0.64%
Odile	4.23%	0.26%	0.0%
Patricia	4.34%	0.05%	0.0%

Table 2: Probabilities of 100-m winds within a 7.5 geodesic degree radius of the case study hurricanes exceeding three critical thresholds. The thresholds are chosen as they represent typical turbine cut-out (25 m s^{-1}), potential structural damage (50 m s^{-1}), and a high possibility of structural damage (70 m s^{-1}).

meteorological records Meyer-Arendt (1991). In early September 1988, a tropical wave moved from West Africa, over the Atlantic ocean, where the warm tropical ocean allowed for tropical cyclone development. By 9 September 1988, the wave had organised into a tropical depression and was named Gilbert. Once over the Caribbean Gilbert intensified rapidly into a Category 3 hurricane and made landfall in Jamaica on 12 September 1988. On 13 September 1988, Gilbert was classified as a Category 5 hurricane, and on 14 September 1988 made landfall on the Yucatan peninsula whilst remaining at this intensity.

During the passage of Gilbert 24–48 hours of cut-out would have been experienced at the YUC site, associated with winds exceeding 25 m s^{-1} (Fig. 4d). Instantaneous wind speeds during this time exceeded 50 m s^{-1} and even exceeded 70 m s^{-1} in the YUC neighbourhood, suggesting that if wind farms had been present at YUC during Hurricane Gilbert, they would have risked structural damage. Gilbert weakened to a Category 3 hurricane as it travelled over the Gulf of Mexico and made landfall again on the northeast coast of Mexico on the 16 September 1988. This would have resulted in 24–48 hours of potential wind farm cut-out at the TMPS site. However, due to the weakening of Hurricane Gilbert by this point, 100-m wind speeds do not exceed the threshold for structural damage (70 m s^{-1}). Hurricane Gilbert is a prime example of how one major hurricane could potentially hinder production at two offshore wind farms within a matter of days.

4.5 Case-study summary

These four case studies have shown that Category 4 and 5 hurricanes have the potential to cause periods of low generation due to wind speed cut-out at all of the proposed OWF sites. Structural damage to the wind farms is also possible, particularly for sites on the Gulf of Mexico coast, as in this case study the Atlantic basin hurricanes have been of stronger intensity (see Fig. 5). All hurricanes would have caused a minimum one hour cut-out at the respective sites. Both Atlantic hurricanes (Gilbert and Wilma) and both Pacific hurricanes (Odile and Patricia) display a similar evolution. For Odile and Patricia, 95% of the 100-m wind speeds are below the 25 m s^{-1} cut-out threshold, and more than 99% of wind speeds are below the 50 m s^{-1} threshold for potential structural damage. These two cases suggest that it is unlikely for a Pacific-born hurricane to result in structural damage to a wind farm. In contrast, during Gilbert and Wilma only 80% of 100-m wind speeds are below the cut-out speed, with 2-3%

chance of potential structural damage (Table 2). For these cases there is a 15% increased chance that cut-out will occur from the passage of an Atlantic born hurricane when compared to those born in the Pacific.

On a more positive note, large areas of wind speeds viable for wind energy generation are also seen associated with these hurricanes (wind up to 25 m s^{-1}). This shows that as well as the potential loss and damage that these storms can cause, they can also lead to times of good generation potential a moderate distance from the TC centres. Therefore, there could also be positive impacts of TCs on wind energy generation (as seen in (Gonçalves et al., 2021) for high impact European wind storms).

Despite the level of detail that can be learned from these case studies, they are only representative examples, and a full multi-decadal assessment is required to confirm which sites are at greatest long-term risk of damage from passing TCs. This is the topic of the next section.

5 Long term hazard assessment

5.1 TC Frequency

We first assess the long term hazard of TCs at potential OWFs by considering the variability in annual frequency of TCs exceeding thresholds of 25 m s^{-1}, representing the typical cut-out speed for a wind turbine, and 50 m s^{-1}, as the maximum extreme wind speed for a Class I wind turbine (Han et al., 2014), in the neighbourhood of each of the four sites. Figure 6a gives an overview of the TC climatology at each of the sites. The IOT reports the highest number of TCs, as that specific location gives rise to the desirable conditions for TC genesis (not shown) before TCs propagate north west away from the IOT Holbach and Bourassa (2014). It should be noted that the majority of the TCs which follow this path stay to the west of the region away from the coast and the shallower ocean, therefore should not negatively impact wind energy generation. BC reports the lowest number of TCs which can be attributed to the influence of the north pacific high as its presence increases wind shear and in turn destroys the vertical structure of TCs before they reach Baja California. Figure 6b illustrates how there are several years where only one site experiences cut-out induced by a TC i.e. 1979, 1985, 1987, 1990, 1992–94, 1999, 2004, 2015, 2018; with no TCs at any site in 1981–1982, 1986 and 1991. Conversely, there is only one year in which all four sites experience a TC exceeding the 25 m s^{-1} (2003) illustrating that the potential detriment caused to the energy sector if all sites were hit in the same year is an unlikely event. TMPS and YUC are both hit by twelve TCs exceeding 50 m s^{-1} from 1979–2019 (see Fig. 6c), with coincident cases only occurring in 1980 and 2005. The year 2005 can be noted as the most active hurricane season before the 2020 season National Oceanic and Atmospheric Administration (2020). While there are several TCs each year at every site (Fig. 6a), there are periods when no TCs exceeding 50 m s^{-1} occurred in the potential OWF neighbourhoods (Fig. 6c). This emphasizes the effect of interannual variability and the need for multiple years of data to be used for wind farm risk assessment, to capture the full range of potential TC related damage.

Table 3: Probability for maximum 10-m wind speed above the indicated thresholds, estimated from maximum wind speeds associated with all TC tracks which enter the vicinity of the potential OWF sites.

Site	> 25 m s^{-1}	> 50 m s^{-1}
Baja California	18.9	0.47
Tamaulipas	27.9	5.46
IOT	17.3	1.59
Yucatan	33.6	5.94

5.2 Wind speed distribution

Figure 7 shows the probability density functions of TC associated maximum 10-m wind speed which occurred in the neighbourhood of the specified region (from IBTrACS 1979–2019). There is no minimum wind speed threshold so all TCs which enter each neighbourhood are included. The probability of a 10-m associated wind speed threshold being met within the neighbourhood is calculated from the data presented in Figure 7 and displayed in Table 3. YUC and TMPS exhibit the highest probability of experiencing cut-out during the passage of a TC at 33.6% and 27.9%, respectively. Furthermore, there is a 5.9% and 5.5% probability that wind speeds greater than 50 m s^{-1} will be experienced at any point within these neighbourhoods, respectively. IOT has a lower probability of exceeding cut-out with 17.3% of wind speeds exceeding 25 m s^{-1}. The low probability of having TC-related wind speeds exceeding 50 m s^{-1} at both IOT (1.6%) and BC (0.5%) can be related to the location of these two sites with respect to the genesis (IOT) and decay (BC) of tropical cyclones as at those two stages in their life-cycles TCs are less likely to sustain extreme wind speeds above this threshold. Note that using 10-m wind speeds (as recorded by IBTrACS) rather than those at 100-m implies that these results give a lower bound for the probabilities, i.e. these would be expected to be higher for 100-m wind speeds.

5.3 TC impact assessment

The return period of TCs making landfall in Mexico is shown in Fig. 8, which also highlights the areas where CF is above 20% during hurricane season (cf. Fig. 2). As expected, regions which are near the coast have a higher probability of being affected by a hurricane, with return periods between 1 and 4 years. However, regions further inland also have a relatively low return period ranging between 1 and 16 years, a result that should be interpreted by recalling that the TC track density was computed using 2 geodesic degree spherical caps, i.e. any TC whose centre passed within approx. 200 km of a given location contributes to the risk attached to that location. When considering landfalling TCs, the four potential OWF sites exhibit return periods between 2 and 4 years, which highlights the coastal risk posed by TCs for a country at a tropical/sub-tropical location. However, this challenge is modulated when considering wind speed above relevant thresholds.

The return periods of TCs with 10-m wind maxima above three different thresholds are

shown in Fig. 9. These return periods have been derived from the TC tracks crossing the neighbourhoods of the four selected sites and estimated using the method described in Section 2.5. The return periods thus obtained are comparable to those estimated for Florida cities Malmstadt et al. (2010). When considering all TCs (Fig. 9(a, d, g, j)) passing through the neighbourhoods of the potential OWF sites, IOT, TMPS and YUC are exposed to similar hazards, with return periods within their neighbourhoods ranging between 2 and 4 years for all but IOT, which exhibits the lowest return period (1 year) among these three sites . This is consistent with the high number of TCs in this area, discussed in Section 5.1. In contrast, BC exhibits longer return periods within its neighbourhood ranging from 2 to 16 years.

Differences between sites become more prominent as the wind speed threshold increases. Considering wind speeds exceeding 25 m s^{-1} (Fig. 9(b, e, h, k)), the sites can be ordered according to their longest return periods, starting with BC, which exhibits the longest return periods between 4 and 64 years and finishing with YUC, which exhibits the shortest return periods between 2 and 8 years. At this wind speed threshold, there is no clear difference between sites on the Pacific coast and those in the Gulf of Mexico. (Fig. 9(c, f, i, j)). However, the return periods for sites on the Pacific coast increase faster with wind speed threshold than those for sites on the Gulf of Mexico. When considering wind speeds exceeding 50 m s^{-1}, the Pacific sites exhibit very long return periods beyond 128 years and 64 years for the cases of BC and IOT, respectively. In contrast, the sites in the Gulf of Mexico exhibit shorter return periods ranging between 8 and 64 years in both cases. Thus, the conclusions drawn from the neighbourhood analysis are consistent with the scenario described by landfalling TCs (Fig. 8), in which the differences seen at high wind speed thresholds between Pacific and Gulf of Mexico sites are due to their location with respect to the typical TC tracks that visit each neighbourhood. As a consequence, the TCs passing through the neighbourhoods of IOT and BC are at the start and end of cyclone tracks, respectively. Therefore, they are less likely to give rise to such high wind speeds. On the other hand, TCs crossing through TMPS and YUC are more likely to be in their maximum intensity phase and, therefore, are more likely to reach damaging wind speeds.

6 Conclusions

The exposure of potential OWFs in Mexico to strong winds related to the passage of TCs has been investigated. The wind energy potential of Mexico during TC season was assessed by estimating CF from 37 years of ERA5-derived 100-m wind speeds. The assessment of the suitability of four potential OWF locations (Baja California, Tamaulipas, Isthmus of Tehuantepec and Yucatan peninsula) was performed through two different approaches. The first consisted of the study of four major hurricanes (Wilma, Gilbert, Patricia and Odile). The second consisted of a return period analysis of historic TCs which have affected these regions. The methodology to carry out the return period analysis was based on the analysis of observed TC tracks under a regional (as opposed to a site-specific) approach to estimate both TC frequency and wind

speed exceedance.

The four selected regions displayed a suitable wind energy potential throughout the year, with CF above 20% on average, in agreement with previous studies Cancino-Solórzano et al. (2011); Gallardo et al. (2020); Jaramillo et al. (2004); Hernández-Escobedo et al. (2010). We have shown that across the four sites there is seasonal variability in CF, which follows the evolution of wind variability Thomas et al. (2020). The greatest degree of variability was found in the IOT site as the seasonal Tehuanos winds accelerate through the gap in the Isthmus topography during the winter months hence producing episodes of high wind speeds. We have also shown that despite this variability the feasibility of all four sites is maintained during the hurricane season (June–November).

The analysis of the four major hurricanes has shown differences between Pacific and Atlantic cyclones at high wind speeds in particular. Thus, while the four hurricanes would have led to periods of low generation due to wind speed cut-out, the Atlantic cyclones were more likely to lead to winds above 50 m s^{-1}. Similarly, the return period analysis has shown clear differences between sites in the Pacific coast and sites in the Gulf of Mexico. The sites in the Gulf of Mexico (TMPS and YUC) would be more frequently impacted by damaging wind speeds with much lower return periods (between 8 and 64 years) than the sites on the Pacific coast (IOT and BC), which exhibit return periods above 64 years.

The findings of this paper are relevant for planning of offshore wind farms in tropical regions in general as the methodology used here would be easily ported to other locations. While these results are based on 40 years of observational data, which is not sufficiently long to consider transient behaviour such as TC clustering or the effects of climate change, the consistency of the results and the observational record has been ensured by suitable statistical hypothesis testing. Nevertheless, incorporating transient effects would constitute a suitable extension to this work, which could be carried out by incorporating more observational data as it is collected and numerical model output. As this work is focused on the meteorological hazard of TCs at sites of potential OWT locations, future work could develop these results into a full risk assessment through incorporating more detailed information on turbine fragility such as in Martín del Campo et al. (2021)).

Acknowledgements

The authors thank Dr K Hodges for the computation, curation and availability of the tropical cyclone tracks derived from both IBTrACS and ERA5 used in this work. This work was funded by the UK Natural Environment Research Council through the National Centre for Atmospheric Science and the Atmospheric hazard in developing Countries: Risk assessment and Early Warning (ACREW) NE/R000034/1 project. OR-H was supported by Mexico CONACyT-SENER-Sustentabilidad Energética, Project 272063, "Strengthening of the field of Wind Energy in the Doctoral Program in Engineering Field of Knowledge in Energy based in the Institute of Renewable Energies of the National Autonomous University of Mexico"

(Institutional Strengthening for Energy Sustainability).

Data Availability

The ERA5 Hersbach et al. (2020) and IBTrACS Knapp et al. (2010) datasets used in this study are available, respectively, at
https://www.ecmwf.int/en/forecasts/datasets/reanalysis-datasets/era5 and
https://www.ncdc.noaa.gov/ibtracs/

References

Barton, E. D., Lavin, M. and Trasviña, A. (2009) Coastal circulation and hydrography in the Gulf of Tehuantepec, Mexico, during winter. *Continental Shelf Research*, **29**, 485–500.

Blanco, M. I. (2009) The economics of wind energy. *Renewable and Sustainable Energy Reviews*, **13**, 1372–1382.

Bloomfield, H. C., Brayshaw, D. J. and Charlton-Perez, A. J. (2020) Characterizing the winter meteorological drivers of the European electricity system using targeted circulation types. *Meteorol. Appl.*, **27**.

Breña-Naranjo, J. A., Pedrozo-Acuña, A., Pozos-Estrada, O., Jiménez-López, S. A. and López-López, M. R. (2015) The contribution of tropical cyclones to rainfall in Mexico. *Phys. Chem. Earth, Parts A/B/C*, **83**, 111–122.

Martín del Campo, J. O., Pozos-Estrada, A. and Pozos-Estrada, O. (2021) Development of fragility curves of land-based wind turbines with tuned mass dampers under cyclone and seismic loading. *Wind Energy*.

Cancino-Solórzano, Y., Gutiérrez-Trashorras, A. J. and Xiberta-Bernat, J. (2011) Current state of wind energy in Mexico, achievements and perspectives. *Renewable and Sustainable Energy Reviews*, **15**, 3552–3557.

Cangialosi, J. and Kimberlain, T. (2015) Hurricane Odile (ep152014). *National Hurricane Center*.

Cannon, A. J., Sobie, S. R. and Murdock, T. Q. (2015a) Bias correction of GCM precipitation by quantile mapping: How well do methods preserve changes in quantiles and extremes? *J. Clim.*, **28**, 6938–6959.

Cannon, D. J., Brayshaw, D. J., Methven, J., Coker, P. J. and Lenaghan, D. (2015b) Using reanalysis data to quantify extreme wind power generation statistics: A 33 year case study in great britain. *Renewable Energy*, **75**, 767–778.

Canul-Reyes, D. (2020) *Feasibility Study of Offshore Wind Energy in the Gulf of Mexico*. Master's thesis, Universidad Nacional Autónoma de México.

Carrasco-Díaz, M., Rivas, D., Orozco-Contreras, M. and Sánchez-Montante, O. (2015) An assessment of wind power potential along the coast of Tamaulipas, northeastern Mexico. *Renewable Energy*, **78**, 295–305.

Chan, J. C. and Kepert, J. D. (2010) *Global perspectives on tropical cyclones: from science to mitigation*. World Scientific.

Clark, G. (1988) Preliminary report hurricane Gilbert: 08–19 september 1988. *1988 Atlantic Hurricane Season: Atlantic Storm Wallet Digital Archives, National Hurricane Centre*.

Clausen, N.-E., Candelaria, A., Gjerding, S., Hernando, S., Nørgård, P., Ott, S. and Tarp-Johansen, N. J. (2007) Wind farms in regions exposed to tropical cyclones. In *2007 European Wind Energy Conference and Exhibition*, vol. 15, 61400–3. European Wind Energy Association (EWEA).

Díaz Méndez, G. M., Lehner, S., Ocampo-Torres, F. J., Ming Li, X. and Brusch, S. (2010) Wind and wave observations off the south Pacific Coast of Mexico using TerraSAR-X imagery. *Int. J. Remote Sens.*, **31**, 4933–4955.

de México Secretaría de Energía, G. (2020) Programa de Desarrollo del Sistema Eléctrico Nacional 2020 -2034.

Franco-Díaz, A., Klingaman, N. P., Vidale, P. L., Guo, L. and Demory, M.-E. (2019) The contribution of tropical cyclones to the atmospheric branch of Middle America's hydrological cycle using observed and reanalysis tracks. *Clim. Dynam.*, **53**, 6145–6158.

Gallardo, R. P., Ríos, A. M. and Ramírez, J. S. (2020) Analysis of the solar and wind energetic complementarity in Mexico. *Journal of Cleaner Production*, **268**, 122323.

Georgiou, P., Davenport, A. G. and Vickery, B. (1983) Design wind speeds in regions dominated by tropical cyclones. *J. Wind Eng. Ind. Aerod.*, **13**, 139–152.

Gkoumas, K. (2010) A risk analysis framework for offshore wind turbines. In *12th Biennial International Conference on Engineering, Construction, and Operations in Challenging Environments*, 1965–1972. Honolulu, Hawaii, USA: ASCE.

Gonçalves, A., Liberato, M. L. and Nieto, R. (2021) Wind energy assessment during high-impact winter storms in southwestern Europe. *Atmosphere*, **12**, 509.

Hallowell, S. T., Myers, A. T., Arwade, S. R., Pang, W., Rawal, P., Hines, E. M., Hajjar, J. F., Qiao, C., Valamanesh, V., Wei, K. et al. (2018) Hurricane risk assessment of offshore wind turbines. *Renewable Energy*, **125**, 234–249.

Han, T., McCann, G., Mücke, T. and Freudenreich, K. (2014) How can a wind turbine survive in tropical cyclone? *Renewable Energy*, **70**, 3–10.

Hernández-Escobedo, Q., Manzano-Agugliaro, F. and Zapata-Sierra, A. (2010) The wind power of Mexico. *Renewable and Sustainable Energy Reviews*, **14**, 2830–2840.

Hersbach, H., Bell, B., Berrisford, P., Hirahara, S., Horányi, A., Muñoz-Sabater, J., Nicolas, J., Peubey, C., Radu, R., Schepers, D. et al. (2020) The ERA5 global reanalysis. *Q. J. R. Meteorol. Soc.*, **146**, 1999–2049.

Hodges, K. (1995) Feature tracking on the unit sphere. *Mon. Weather Rev.*, **123**, 3458–3465.

— (1999) Adaptive constraints for feature tracking. *Mon. Weather Rev.*, **127**, 1362–1373.

Hodges, K., Cobb, A. and Vidale, P. L. (2017) How well are tropical cyclones represented in reanalysis datasets? *J. Clim.*, **30**, 5243–5264.

Hodges, K. I. (1994) A general method for tracking analysis and its application to meteorological data. *Mon. Weather Rev.*, **122**, 2573–2586.

Holbach, H. M. and Bourassa, M. A. (2014) The effects of gap-wind-induced vorticity, the monsoon trough, and the ITCZ on east pacific tropical cyclogenesis. *Mon. Weather Rev.*, **142**, 1312–1325.

Hong, L. and Möller, B. (2012) An economic assessment of tropical cyclone risk on offshore wind farms. *Renewable Energy*, **44**, 180–192.

Hurd, W. E. (1929) Northers of the Gulf of Tehuantepec. *Mon. Weather Rev.*, **57**, 192–194.

Jaimes, M. A., García-Soto, A. D., Martín del Campo, J. O. and Pozos-Estrada, A. (2020) Probabilistic risk assessment on wind turbine towers subjected to cyclone-induced wind loads. *Wind Energy*, **23**, 528–546.

Jaimes, M. A. and Niño, M. (2018) Probabilistic wind risk assessment induced by hurricanes on economically vulnerable households in Mexico. *Natural Hazards Review*, **19**, 04018012.

Jaramillo, O., Saldaña, R. and Miranda, U. (2004) Wind power potential of Baja California Sur, Mexico. *Renewable Energy*, **29**, 2087–2100.

Jáuregui, E. (2003) Climatology of landfalling hurricanes and tropical storms in Mexico. *Atmósfera*, **16**, 193–204.

Katz, R. W. (2002) Stochastic modeling of hurricane damage. *J. Appl. Meteorol. Clim.*, **41**, 754–762.

Kimberlain, T., Blake, E. S. and Cangialosi, J. P. (2016) Tropical cyclone report: Hurricane Patricia (ep202015). *National Hurricane Center*.

Knapp, K. R., Kruk, M. C., Levinson, D. H., Diamond, H. J. and Neumann, C. J. (2010) The international best track archive for climate stewardship (IBTrACS) unifying tropical cyclone data. *B. Am. Meteorol. Soc.*, **91**, 363–376.

Kruk, M. C., Knapp, K. R. and Levinson, D. H. (2010) A technique for combining global tropical cyclone best track data. *J. Atmos. Ocean Tech.*, **27**, 680–692.

Maldonado, T., Alfaro, E. J. and Hidalgo, H. G. (2018) A review of the main drivers and variability of Central America's climate and seasonal forecast systems. *Rev. Biol. Trop.*, **66**, S153–S175.

Malhotra, S. (2007) Design and construction considerations for offshore wind turbine foundations. In *International Conference on Offshore Mechanics and Arctic Engineering*, vol. 42711, 635–647.

Malmstadt, J. C., Elsner, J. B. and Jagger, T. H. (2010) Risk of strong hurricane winds to Florida cities. *J. Appl. Meteorol. Clim.*, **49**, 2121–2132.

Martínez Narro, G., Henshaw, P. F. and Ting, D. S.-K. (2014) Mexico's shoreline as a site for the transition to renewable energy. *Int. J. Environ. Stud.*, **71**, 877–886.

Meyer-Arendt, K. J. (1991) Hurricane Gilbert: The storm of the century. *GeoJournal*, **23**, 323–325.

Morales-Ruvalcaba, C. F., Rodriguez-Hernandez, O., Martínez-Alvarado, O., Drew, D. R. and Ramos, E. (2020) Estimating wind speed and capacity factors in mexico using reanalysis data. *Energy Sustain. Dev.*, **58**, 158–166.

Murià-Vila, D., Jaimes, M. Á., Pozos-Estrada, A., López, A., Reinoso, E., Chávez, M. M., Peña, F., Sánchez-Sesma, J. and López, O. (2018) Effects of hurricane Odile on the infrastructure of Baja California Sur, Mexico. *Natural Hazards*, **91**, 963–981.

National Oceanic and Atmospheric Administration (2020) Record-breaking atlantic hurricane season draws to an end. https://www.noaa.gov/media-release/record-breaking-atlantic-hurricane-season-draws-to-end. Accessed 21 April 2021.

Neumann, C. (2017) A global tropical cyclone climatology. In *Global guide to tropical cyclone forecasting*, WMO-No. 1194, 28–62. World Meteorological Organization. URL: `https://library.wmo.int/doc_num.php?explnum_id=5736`.

Olauson, J. (2018) ERA5: The new champion of wind power modelling? *Renewable Energy*, **126**, 322–331.

Parisi, F. and Lund, R. (2008) Return periods of continental US hurricanes. *J. Clim.*, **21**, 403–410.

Pasch, R. J., Blake, E. S., Cobb III, H. D. and Roberts, D. P. (2006) Tropical cyclone report: Hurricane Wilma, 15–25 October 2005. *National Hurricane Center*, **12**.

Prósper, M. A., Sosa Tinoco, I., Otero-Casal, C. and Miguez-Macho, G. (2019) Downslope windstorms in the Isthmus of Tehuantepec during Tehuantepecer events: a numerical study with WRF high-resolution simulations. *Earth Syst. Dynam.*, **10**, 485–499.

Quaschning, V. V. (2019) *Renewable energy and climate change*. John Wiley & Sons.

Roberts, J., Champion, A., Dawkins, L., Hodges, K., Shaffrey, L., Stephenson, D., Stringer, M., Thornton, H. and Youngman, B. (2014) The XWS open access catalogue of extreme European windstorms from 1979 to 2012. *Nat. Hazard. Earth Sys.*, **14**, 2487–2501.

Rogers, R. F., Aberson, S., Bell, M. M., Cecil, D. J., Doyle, J. D., Kimberlain, T. B., Morgerman, J., Shay, L. K. and Velden, C. (2017) Rewriting the tropical record books: The extraordinary intensification of Hurricane Patricia (2015). *B. Am. Meteorol. Soc.*, **98**, 2091–2112.

Simpson, R. H. and Riehl, H. (1981) *The hurricane and its impact*. Louisiana State University Press.

Steenburgh, W. J., Schultz, D. M. and Colle, B. A. (1998) The structure and evolution of gap outflow over the Gulf of Tehuantepec, Mexico. *Mon. Weather Rev.*, **126**, 2673–2691.

Taylor, H. T., Ward, B., Willis, M. and Zaleski, W. (2010) The Saffir-Simpson hurricane wind scale. *Atmospheric Administration: Washington, DC, USA*.

Thomas, S. R., Martínez-Alvarado, O., Drew, D. and Bloomfield, H. (2020) Drivers of extreme wind events in Mexico for windpower applications. *Int. J. Climatol.*

Wang, Y.-q. and Wu, C.-C. (2004) Current understanding of tropical cyclone structure and intensity changes–a review. *Meteorology and Atmospheric Physics*, **87**, 257–278.

Wilks, D. S. (2011) *Statistical methods in the atmospheric sciences*. Amsterdam: Academic Press, Elsevier, 3rd edn.

Worsnop, R. P., Lundquist, J. K., Bryan, G. H., Damiani, R. and Musial, W. (2017) Gusts and shear within hurricane eyewalls can exceed offshore wind turbine design standards. *Geophys. Res. Lett.*, **44**, 6413–6420.

Zhang, X., Wang, M., Wang, Y. and Liu, Y. (2018) Research on failure of offshore wind turbine tower in typhoon. In *2018 OCEANS-MTS/IEEE Kobe Techno-Oceans (OTO)*, 1–4. IEEE.

Figure 1: Regions in Mexico identified as wind potential zones for power production. Baja California Peninsula (BC, western peninsula), Tamaulipas (TMPS, northeastern coast), Isthmus of Tehuantepec (IOT, southeast coast) and Yucatan peninsula (YUC, eastern peninsula).

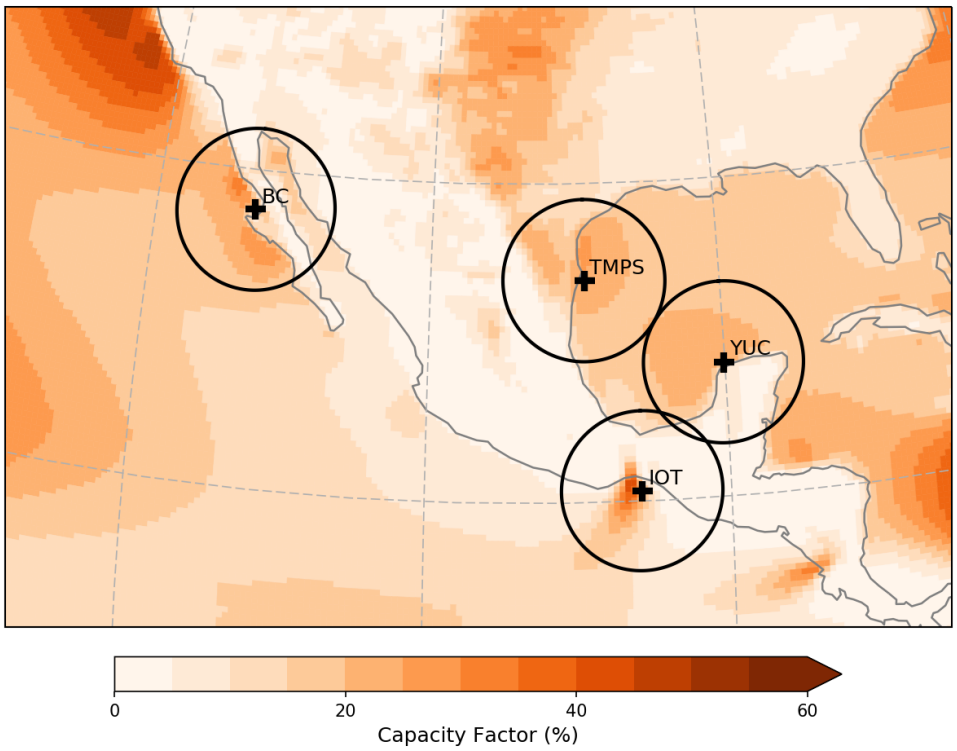

Figure 2: Mean CF for a class I wind turbine (Enercon E70 2.3MW) during hurricane season (1 June–30 November) derived from ERA5 100-m wind speed for the period between 1 January 1980 and 31 December 2017. The black circles represent 3.8 geodesic degree spherical caps centred around hypothetical OWF locations: BC, TMPS, IOT, and YUC.

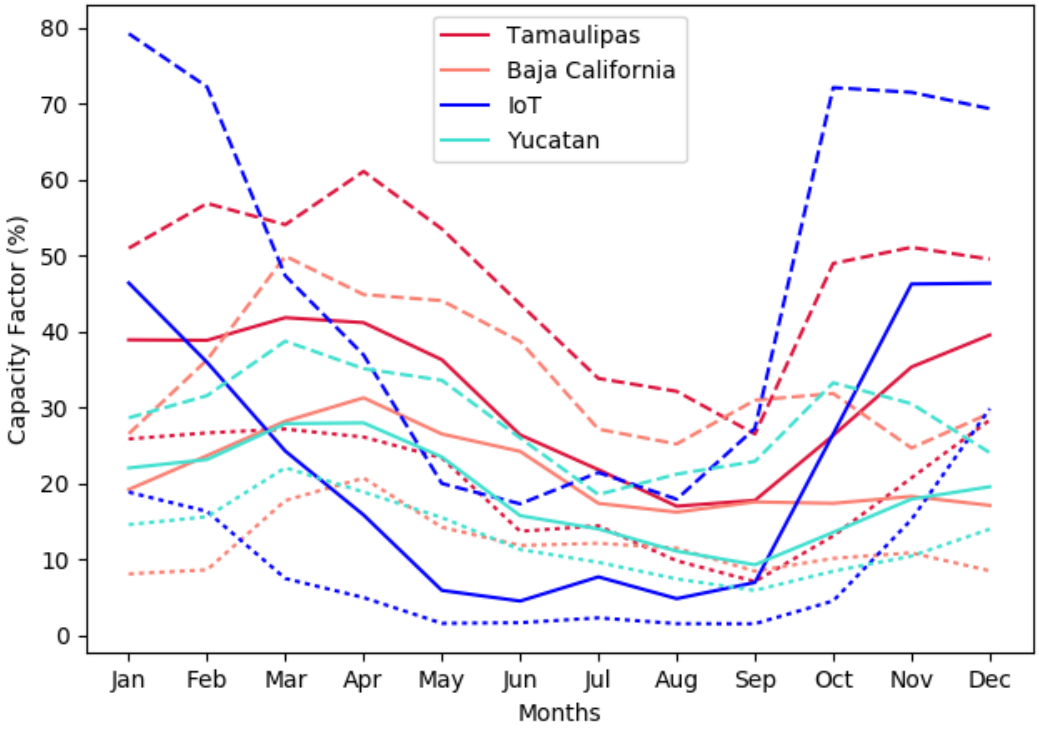

Figure 3: Annual evolution of minimum (dotted lines), median (solid lines) and maximum (dashed lines) mean monthly CFs for a class I wind turbine (Enercon E70 2.3MW) at the hypothetical OWF locations derived from ERA5 100-m wind speed for the period between 1 January 1980 and 31 December 2017.

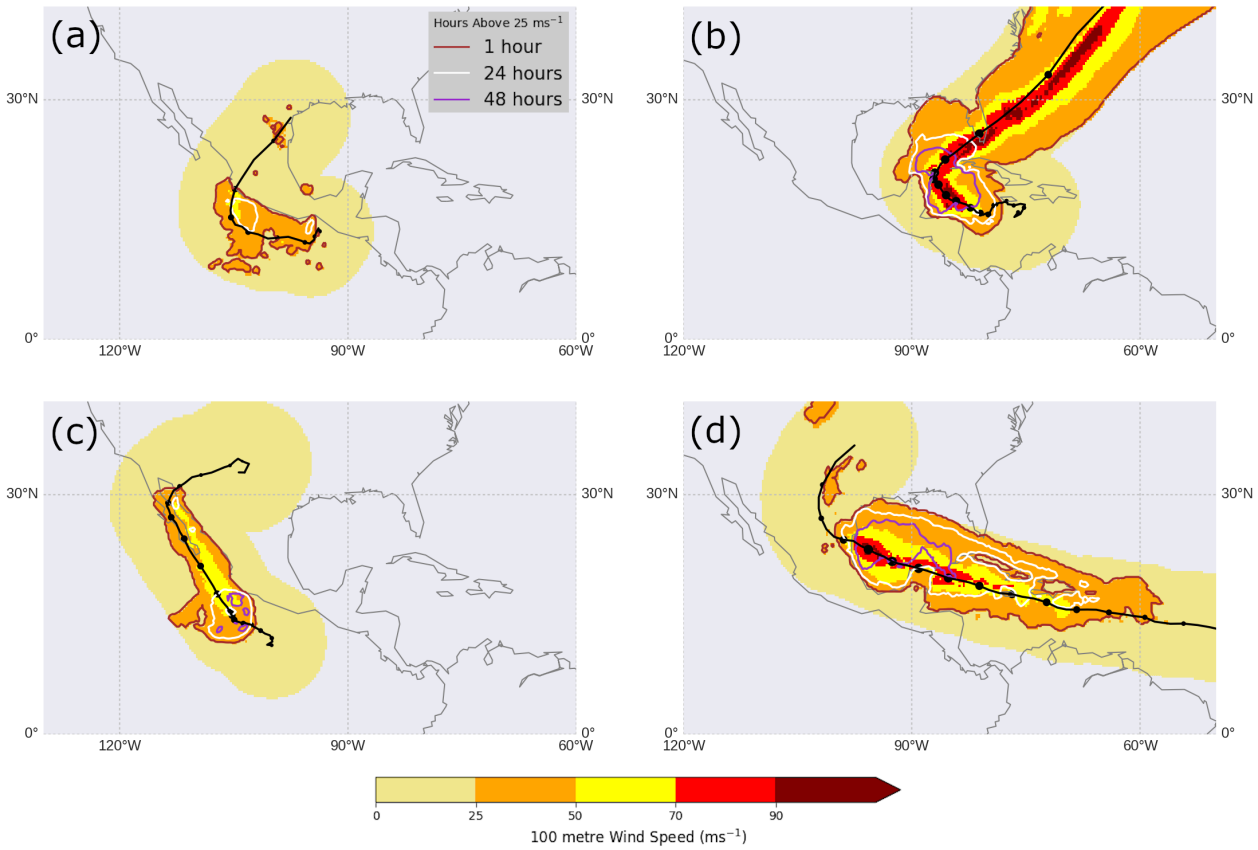

Figure 4: Wind speed footprints of hurricanes (a) Patricia, (b) Wilma, (c) Odile and (d) Gilbert, based on bias-corrected ERA5 100-m wind speed. The solid black line represents the cyclone track and the black dot size is proportional to the maximum vorticity. Shaded contours show the maximum 100-m wind speed reached during the hurricane. Coloured line contours represent the number of hours experienced above the turbine cut-out speed (25 m s^{-1}) during the hurricane's life cycle.

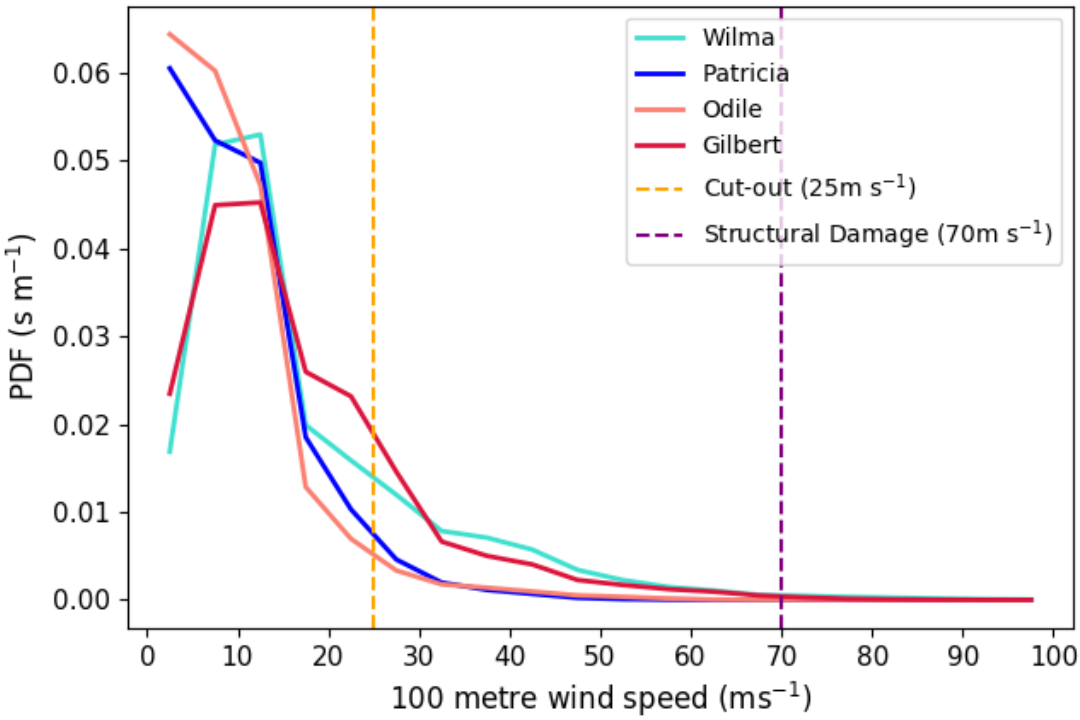

Figure 5: Probability distribution function of 100-m winds within a 7.5 geodesic degree radius of the case study hurricane tracks (see Figure 4). The dashed yellow line represents the typical turbine cut-out (25 m s^{-1}) and the black dashed line represents the wind speed at which there is a high chance of structural damage (70 m s^{-1}).

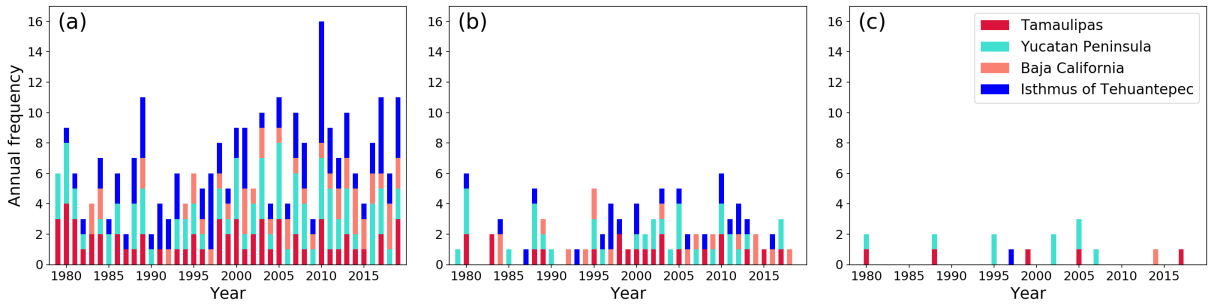

Figure 6: Number of TCs in each region between 1979 and 2019 at different 10-m wind speed thresholds as recorded by IBTrACS: a $w > 0$ m s^{-1} (all TCs), (b) $w > 25$ m s^{-1}, and (c) $w > 50$ m s^{-1}.

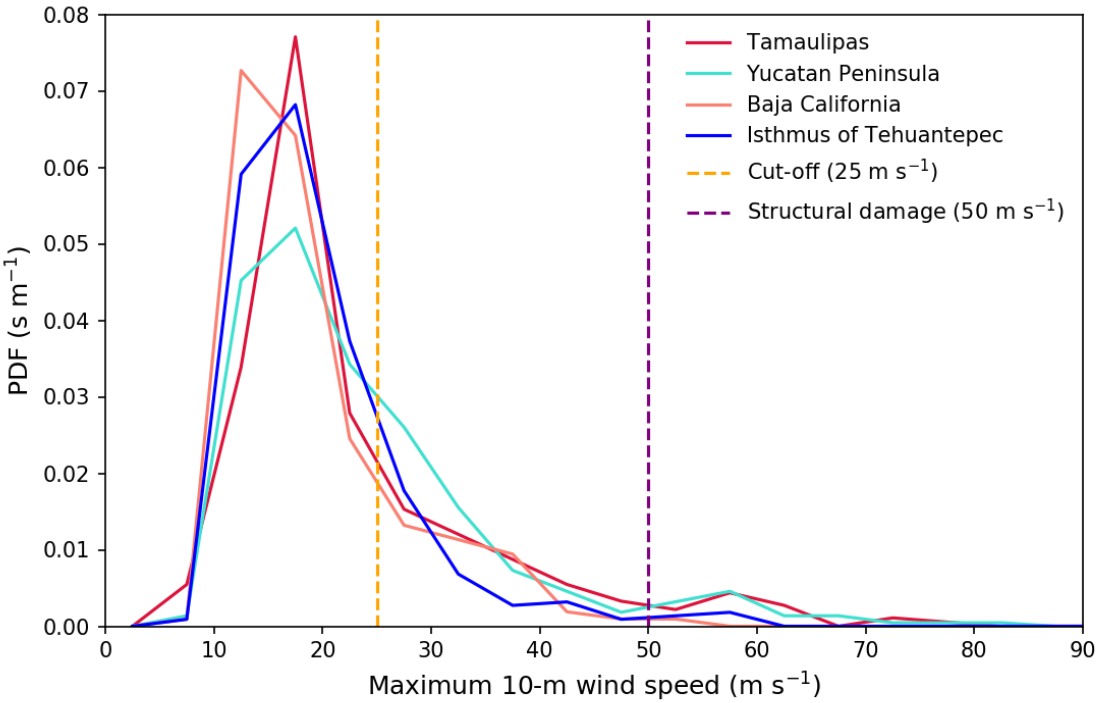

Figure 7: Probability density functions of maximum 10-m wind speed, as recorded by IB-TrACS between 1979 and 2019, associated with the passage of TCs in the neighbourhood of the hypothetical OWFs. The dashed yellow line represents the typical turbine cut-out (25 ms^1). The purple dashed line represents the wind speed at which there is an increased chance of structural damage (50 m s^{-1}).

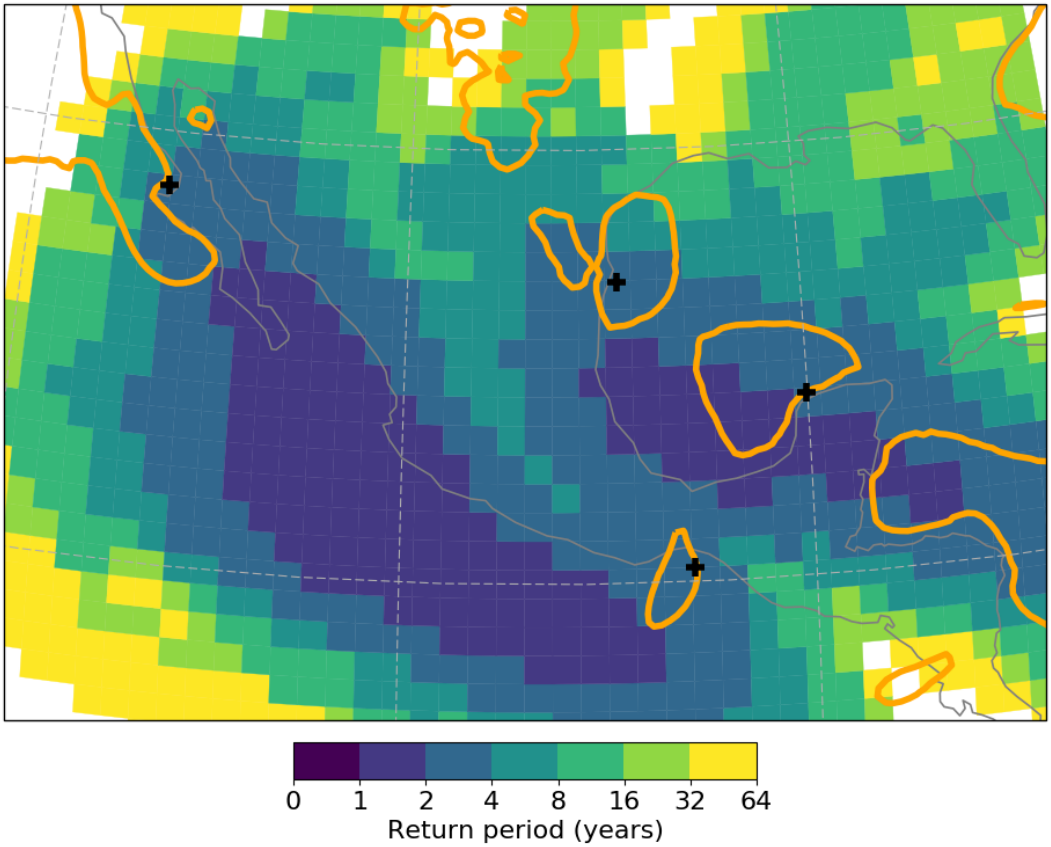

Figure 8: Return period, in years, of TCs making a landfall in Mexico. The orange contours represent a CF of 20% during hurricane season (cf. Fig. 2). The black crosses represent the potential OWF locations.

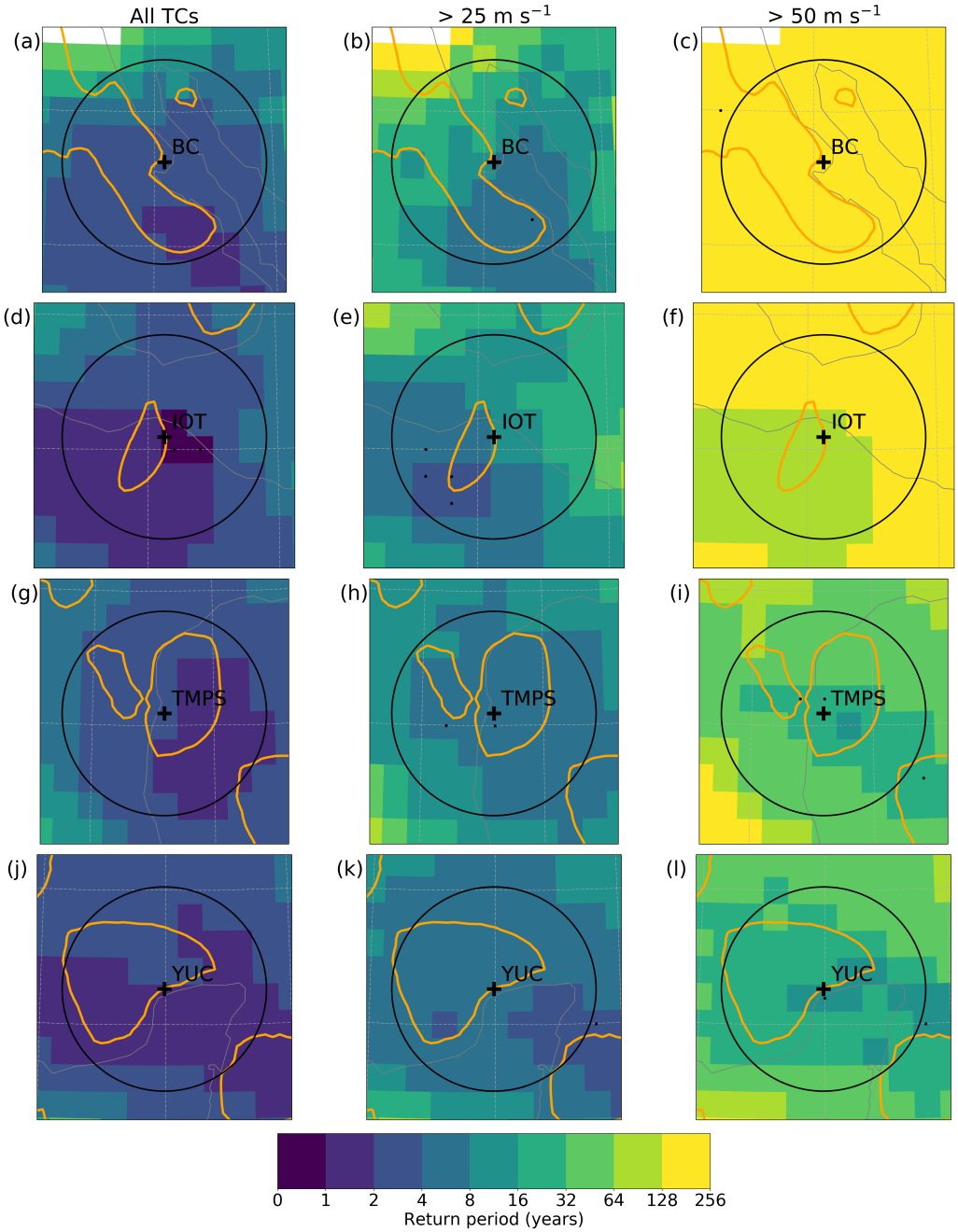

Figure 9: Return period, in years, of TCs with maximum 10-m wind speed exceeding (a, d, g, j) 0 m s^{-1} (all TCs), (b, e, h, k) 25 m s^{-1} and (c, f, i, l) 50 m s^{-1}, around the neighbourhood of (a–c) Baja California (BC), (d–f) Tamaulipas (TMPS), (g–h) the Isthmus of Tehuantepec (IOT) and (j–l) Yucatan (YUC). The orange contours represent a mean CF of 20% during hurricane season. The black crosses represent the hypothetical OWF sites and the black circles represent 3.8-geodesic degree neighbourhoods centred at the sites. Stippling indicates grid points for which the return period calculation is not significant at the 10% significance level.